Title page

Instability of a class A GPCR oligomer interface

Jacqueline M. Fonseca and Nevin A. Lambert

Department of Pharmacology and Toxicology, Medical College of Georgia, Augusta, GA 30912, USA.

1

Running title page

a)   Running title: Instability of a GPCR oligomer interface

b)   Correspondence should be addressed to:

Nevin Lambert

Department of Pharmacology and Toxicology

Medical College of Georgia

Augusta, GA 30912-2300

Voice: 706-721-6336

Fax: 706-721-2347

nlambert@mcg.edu

c)   number of text pages: 13

number of tables: 0

number of figures: 3

number of references: 12

number of words in abstract: 159

number of words in introduction: 292

number of words in discussion: 332

d)   Nonstandard abbreviations: GPCR, G protein-coupled receptor; TM, transmembrane domain; FRAP, fluorescence recovery after photobleaching; CuP; Cu^{2+}(phenanthroline)$_2$; CFP, cyan fluorescent protein; V, venus.

Abstract:

The quaternary structure of G protein-coupled receptors (GPCRs) can influence their trafficking and ability to transduce signals. GPCR oligomers are generally portrayed as long-lived entities, although the stability of these complexes has not been studied. Here we show that D2 dopamine receptor protomers interact transiently at a specific oligomer interface. Selective immobilization of CFP-D2 receptors (C-D2R) in the plasma membrane failed to completely immobilize coexpressed D2-venus receptors (D2R-V), suggesting the two did not form stable oligomers with each other. Oxidative crosslinking stabilized C-D2R-D2R-V oligomers such that immobilization of C-D2R also immobilized D2R-V. This stabilization required the presence in both C-D2R and D2R-V of a cysteine residue in transmembrane domain 4 (TM4), a region identified as a putative oligomer interface in these and other class A GPCRs. These results suggest that the interaction of D2 receptor protomers at TM4 is transient unless stabilized, and that the quaternary structure of these receptors may thus be subject to physiological or pharmacological regulation.

Introduction:

GPCRs can exist and function in cells as dimers or higher-order oligomers (Bouvier, 2001; Milligan, 2007). However, the structural arrangement of GPCR protomers within oligomers and the dynamics of oligomer assembly and disassembly are not well-understood (Gurevich and Gurevich, 2008). The most is known about class C (metabotropic glutamate-like) oligomers; the interfaces between class C protomers involve either extracellular disulfide bonds or intracellular coiled-coils and are thought to be relatively stable (Bouvier, 2001). By comparison, the interfaces between class A (rhodopsin-like) protomers are poorly-defined, although it is likely that transmembrane regions are involved. Transmembrane class A interfaces identified by molecular models and crystallography occupy relatively small protein surfaces (Liang et al., 2003; Lodowski et al., 2007), suggesting that oligomers formed at these interfaces might not be stable. However, it is difficult to predict class A GPCR oligomer stability because these interfaces are buried in a hydrophobic environment, and because the proteins are concentrated in a two-dimensional membrane.

   To directly assess the stability of a class A GPCR oligomer interface we selectively immobilized a subset of protomers on the surface of cells using specific antibodies. The lateral mobility of non-crosslinked protomers was then measured using fluorescence recovery after photobleaching (FRAP). The mobility of non-crosslinked protomers should have been decreased if these protomers formed stable oligomers with antibody-crosslinked protomers. We chose to study D2 dopamine receptors because oxidative crosslinking studies have identified the fourth transmembrane helix (TM4) of this receptor as part of a conformationally-sensitive homooligomer interface (Guo et al., 2005; Guo et al., 2003). TM4 (together with TM5) has also been identified as an interface between protomers of rhodopsin and other class A GPCRs (Gonzalez-Maeso et al., 2008; Kota et al., 2006), thus this helix may be a general class A oligomer interface.

Materials and Methods

Molecular Biology. D2R-V was generously provided by Dr. Jonathan Javitch (Columbia University College of Physicians and Surgeons, New York, NY). This construct lacks three native cysteine residues (C118S/C371S/C373S), none of which is located at the putative TM4 interface. C-D2R was constructed by amplifying D2R from D2R-V and inserting this fragment behind a signal sequence from human growth hormone and enhanced cyan fluorescent protein (ECFP) using the PCR. β2AR-V was constructed by fusing venus to the c-terminus of the human β2AR. The transmembrane domain in C-TM-V and C-TM was the first transmembrane domain from the human μ opioid receptor. All constructs were verified by automated sequencing.

Cell Culture and Transfection. HEK 293 cells (ATCC) were plated on poly-L-lysine-coated coverslips in 6-well tissue culture plates and cultured in MEM supplemented with 10% FBS for 24-48 hours prior to transfection. Cells that were 50% to 70% confluent were transfected with a 5:1 ratio of plasmid DNA encoding C-D2R and D2R-V using polyethylenimine. Cells were used for experiments 12-24 hours after transfection.

Antibody and oxidative crosslinking. Medium was removed from cells and washed 3 times with buffer containing (in mM): 150 NaCl, 10 NaHEPES, 12.8 d-glucose, 2.5 KCl, 0.5 $MgCl_2$, and 0.5 $CaCl_2$ (pH 8.0) at room temperature. For antibody crosslinking cells were incubated sequentially for 5 minutes each (separated by 3 buffer washes) in 1:200 anti-GFP rabbit IgG (Invitrogen) and biotin-XX goat anti-rabbit (Invitrogen). For oxidative crosslinking cells were first incubated for 10 minutes in a solution containing 1 mM $CuSO_4$ and 2 mM 1,10-phenanthroline (CuP), washed in buffer 3 times, then crosslinked with antibodies as described above. Control cells in these experiments were incubated in CuP-free buffer for the equivalent time prior to antibody crosslinking.

Imaging and fluorescence recovery after photobleaching. FRAP experiments were performed at room temperature on the stage of an inverted Leica SP2 laser scanning confocal microscope. ECFP and venus excitation intensities were standardized by setting an acuousto-optic tunable filter to allow transmission of 6% of the 458 nm laser line and 1% of the 514 nm laser line (or an equivalent ratio of these two lines) to reach the specimen; ECFP and venus emissions were sampled at 460-500 nm and 520-700 nm, respectively. After scanning at low power for 10 seconds a 5 μm circular region of

interest (ROI) was photobleached with a single scan at high power (75-100% transmission), after which scanning was resumed at low power for 180 seconds. Background-subtracted average intensity in a sub-ROI containing the bleached plasma membrane was divided by a control ROI to correct for bleaching during low power scanning. Recovery was defined as the fractional recovery after 180 seconds.

Immunoblotting. Transfected cells plated on poly-L-lysine-coated 100mm cell culture dishes were washed twice with PBS and incubated for 10 minutes in either PBS or CuP (see above). After washing cells were then incubated for 20 minutes at RT in a solution containing PBS supplemented with 1 mM $CaCl_2$ and 0.1 mM $MgCl_2$, 20 mM N-ethylmaleimide (NEM), and protease inhibitor cocktail (Sigma). Cells were scraped on ice, centrifuged at 1,500 rpm, 4 °C, for 5 minutes and lysed in 1% dodecylmaltopyranoside containing 20 mM NEM. Extracts were isolated by centrifugation at 20,000 rpm, 4 °C for 30 minutes, and total protein concentration was measured using BCA Protein Assay (Pierce). Equal amounts of protein were mixed with an equal volume of non-reducing 2X sample buffer and warmed to 37 °C for 15 minutes. Proteins were resolved on 4-20% gradient SDS-PAGE precast gels (Pierce) and transferred onto PVDF membrane. Membranes were probed with anti-GFP rabbit IgG (1:1000) and HRP-conjugated anti-rabbit (Pierce; 1:10,000). Proteins were detected using enhanced chemiluminescence (SuperSignal West Pico; Pierce).

Electrophysiology and data analysis. Whole-cell voltage-clamp recordings were made using standard procedures from transfected cells on the stage of an inverted fluorescence microscope. Cells were held at a membrane potential of -60 mV, and were stepped to -100 mV for 0.2 s, and then ramped from -100 to 0 mV at a rate of 0.18 mV ms^{-1}. Electrodes (4-5 MΩ) were filled with a solution containing 140 mM K-gluconate, 5 mM KCl, 0.2 mM EGTA, 10 mM HEPES, 3 mM MgATP, 0.3 mM Na_2GTP (pH 7.2, ~295 mOsm kg^{-1} H_2O). Cells were perfused with a solution containing 122.5 or 150 mM NaCl, 30 mM or 5mM KCl, 10 mM HEPES, 10 mM glucose, 1.5 mM $CaCl_2$, and 2.5 mM $MgCl_2$ (pH 7.2, ~320 mOsm kg^{-1} H_2O). Solution changes were made using a multiport attachment and perfusion capillary positioned directly in front of the cell under study. Statistical comparisons were made using the unpaired t-test; $P<0.001$ was considered statistically significant.

Results:

Enhanced cyan fluorescent protein (ECFP; C) and the yellow fluorescent protein venus (V) were fused to the extracellular N-terminus and intracellular C-terminus, respectively, of a cysteine-depleted D2 receptor used in previous studies of the TM4 interface (Guo et al., 2005; Guo et al., 2003). When expressed in HEK 293 cells these fusion proteins (C-D2R and D2R-V) trafficked to the plasma membrane and adopted the expected orientation (Fig. 1*A, B*). The C moiety of C-D2R was extracellular and the V moiety of D2R-V was intracellular, as shown by immunostaining of intact cells with an anti-GFP antibody (Fig. 1*A*) and susceptibility to trypsin digestion (Fig. 1*B*). C-D2R and D2R-V were both functional, as shown by activation of inwardly-rectifying potassium channels (C-D2R, 167 ± 32 pA, *n*=7; D2R-V, 352 ± 62 pA, *n*=6; no-receptor control, 17 ± 9 pA, *n*=5).

C-D2R and D2R-V were coexpressed under conditions such that C-D2R were more abundant than D2R-V in most cells, with the expectation that this mismatch would favor assembly of D2R-V-containing oligomers that also contained a C-D2R protomer. Cells were selected for imaging based on the relative intensities of C-D2R and D2R-V. The ratio of C-D2R and D2R-V expression in these same cells was measured by calibrating C and V intensity at the cell surface with a standard, fixed-stoichiometry transmembrane protein (C-TM-V; Fig. 1*C, D*). With standardized imaging conditions the C:V intensity ratio at the plasma membrane was 0.60 ± 0.02 (*n*=30) for C-TM-V and 3.05 ± 0.16 (*n*=103) for coexpressed C-D2R and D2R-V, thus the average C-D2R:D2R-V expression ratio in the cells studied was ~5:1.

The lateral mobilities of coexpressed C-D2R and D2R-V were then measured with FRAP. The rates of fluorescence recovery were indistinguishable for these two receptors (Fig. 2*A*, *B*), suggesting that the dimensions of the transmembrane elements of both proteins (or oligomers containing them) were similar. C-D2R at the cell surface were crosslinked by sequential incubation of live cells with a polyclonal anti-GFP antibody and a secondary antibody. Antibody crosslinking virtually immobilized C-D2R, as indicated by a dramatic decrease in fluorescence recovery after photobleaching (Fig. 2*A*, *C*). The antibodies used for crosslinking had no access to the V moiety of D2R-V, yet crosslinking would be expected to also immobilize these protomers if they formed stable

oligomers with C-D2R. In contrast, antibody crosslinking had a relatively modest effect on D2R-V mobility (Fig. 2*B*, *C*). Activation of C-D2R and D2R-V with the agonist quinpirole had no effect on D2R-V mobility after antibody crosslinking (*P*=0.82; *n*=7). In order to determine if the effect of antibody crosslinking on D2R-V mobility reflected a specific protein interaction, we performed the analogous experiment with C-D2R and a β2-adrenoreceptor-venus fusion (β2AR-V), a protein that is not known to interact with D2Rs. Antibody crosslinking of C-D2R had a similar effect on the mobility of β2AR-V (Fig. 2*D*) when the two were expressed at relative levels similar to C-D2R and D2R-V (C:V intensity ratio = 3.94 ± 0.42; *n*=31). This suggested that the slowing of D2R-V mobility by immobile C-D2R was not entirely specific. In fact, we found that antibody crosslinking of even a single-TM control protein (C-TM) decreased D2R-V mobility (Fig. 2*E*; C:V intensity ratio = 4.98 ± 1.06; *n*=18). This suggests that immobile TM proteins may non-specifically decrease the lateral mobility of other TM proteins, which is consistent with previous reports that membrane protein crowding decreases the lateral mobility of transmembrane proteins (Frick et al., 2007). We can not rule out an alternative possibility, namely that these control proteins interact with D2Rs in a manner similar to the interaction of C-D2R and D2R-V with each other.

The mobility of D2R-V after selective crosslinking of C-D2R implied that the majority of these protomers did not reside in stable oligomers that also contained a C-D2R protomer. Thus either C-D2R and D2R-V did not form heterooligomers at all, or else C-D2R-D2R-V heterooligomers were not stable. The TM4 interface between D2R protomers can be stabilized by oxidative crosslinking of either native or introduced cysteine residues (Guo et al., 2005; Guo et al., 2003). We reasoned, therefore, that oxidative crosslinking would stabilize this interaction if C-D2R and D2R-V protomers could associate at the TM4 interface. We verified that both receptors (expressed at a 1:1 ratio) migrated as monomers on non-reducing SDS-PAGE, and that treatment of intact cells with the oxidizing reagent Cu^{2+}(phenanthroline)$_2$ (CuP) induced the formation of SDS-resistant dimers (Fig. 3*A*). CuP did not induce C-D2R or D2R-V dimers when cysteine 168 in TM4 was mutated to serine, as shown previously for D2R (Fig. 3*A*). We then measured C-D2R and D2R-V mobility in cells that were crosslinked with antibodies alone or with antibodies and CuP. Immobilization of C-D2R was not changed by

8

oxidative crosslinking (c.f. Fig. 2*C* and Fig. 3*D*). However, immobile C-D2R produced a significantly greater slowing of D2R-V mobility in CuP-treated cells than in untreated controls ($P<0.001$; Fig. 3*D*). Fluorescence recovery of D2R-V in CuP-treated cells was similar to that of C-D2R, suggesting that these protomers formed highly stable heterooligomers after oxidative crosslinking. In contrast, CuP did not enhance immobilization of D2R-V when either C-D2R or D2R-V incorporated a serine residue at position 168 (S168; Fig. 2*E*, *F*). This result rules out a non-specific effect of CuP on D2R-V mobility mediated by factors intrinsic to the cells, and specifically indicates the involvement of TM4 in the formation of stable C-D2R-D2R-V heterooligomers after oxidative crosslinking. These results suggest that C-D2R and D2R-V could interact at the TM4 interface in these experiments, but that this interaction was transient unless it was stabilized by oxidative crosslinking.

Discussion:

The quaternary structure of GPCRs has been studied extensively. Oligomerization has been shown to alter GPCR trafficking and function, and in some cases oligomers possess unique pharmacological or signaling properties (Park and Palczewski, 2005). However, the structural elements involved in oligomerization and the stability of oligomers are largely unknown (Gurevich and Gurevich, 2008). The possibility that GPCR oligomers might be short-lived entities in the plasma membrane has not been explored, perhaps because few experimental methods can measure the stability of multiprotein complexes in the plasma membrane of live cells. Here we utilized a method whereby selective immobilization of one component of such complexes provides a simple means to assess association of other components. Using this method we have shown that at least one GPCR oligomer interface is relatively unstable, to the point where immobile protomers (C-D2R) have no detectable specific effect on the mobility of other protomers (D2R-V). Thus the lifetime of D2R oligomers joined at the TM4 interface must be short relative to the time scale of macroscopic diffusion. This does not imply that D2R protomers interact randomly at this interface, as biologically-significant protein-protein interactions can be transient. Higher resolution methods will be required to determine the absolute stability of D2R interactions at TM4. We also wish to emphasize that our results do not rule out the possibility that C-D2R and D2R-V form more stable homooligomers at another interface (Guo et al., 2008). For example, we can not rule out the possibility that mobile D2R-V exists partly or entirely as stable D2R-V-D2RV homooligomers. However, if this is the case, these oligomers do not interface at TM4. It is important to consider the possibility that GPCR oligomers need not be highly stable in order to function as oligomers. For example, transient oligomerization might facilitate exchange of protomers during receptor activation (Guo et al., 2005). If class A GPCR oligomers in general are not highly stable, then the dynamics of oligomer association and dissociation may be subject to physiological regulation or pharmacological intervention.

Acknowledgements

References

Bouvier M (2001) Oligomerization of G-protein-coupled transmitter receptors. *Nat Rev Neurosci* **2**(4):274-286.

Frick M, Schmidt K and Nichols BJ (2007) Modulation of lateral diffusion in the plasma membrane by protein density. *Curr Biol* **17**(5):462-467.

Gonzalez-Maeso J, Ang RL, Yuen T, Chan P, Weisstaub NV, Lopez-Gimenez JF, Zhou M, Okawa Y, Callado LF, Milligan G, Gingrich JA, Filizola M, Meana JJ and Sealfon SC (2008) Identification of a serotonin/glutamate receptor complex implicated in psychosis. *Nature* **452**(7183):93-97.

Guo W, Shi L, Filizola M, Weinstein H and Javitch JA (2005) Crosstalk in G protein-coupled receptors: changes at the transmembrane homodimer interface determine activation. *Proc Natl Acad Sci U S A* **102**(48):17495-17500.

Guo W, Shi L and Javitch JA (2003) The fourth transmembrane segment forms the interface of the dopamine D2 receptor homodimer. *J Biol Chem* **278**(7):4385-4388.

Guo W, Urizar E, Kralikova M, Mobarec JC, Shi L, Filizola M and Javitch JA (2008) Dopamine D2 receptors form higher order oligomers at physiological expression levels. *The EMBO journal* **27**(17):2293-2304.

Gurevich VV and Gurevich EV (2008) How and why do GPCRs dimerize? *Trends in pharmacological sciences* **29**(5):234-240.

Kota P, Reeves PJ, Rajbhandary UL and Khorana HG (2006) Opsin is present as dimers in COS1 cells: identification of amino acids at the dimeric interface. *Proc Natl Acad Sci U S A* **103**(9):3054-3059.

Liang Y, Fotiadis D, Filipek S, Saperstein DA, Palczewski K and Engel A (2003) Organization of the G protein-coupled receptors rhodopsin and opsin in native membranes. *J Biol Chem* **278**(24):21655-21662.

Lodowski DT, Salom D, Le Trong I, Teller DC, Ballesteros JA, Palczewski K and Stenkamp RE (2007) Reprint of "Crystal packing analysis of Rhodopsin crystals" [J. Struct. Biol. 158 (2007) 455-462]. *J Struct Biol* **159**(2):253-260.

Milligan G (2007) G protein-coupled receptor dimerisation: molecular basis and relevance to function. *Biochim Biophys Acta* **1768**(4):825-835.

Park PS and Palczewski K (2005) Diversifying the repertoire of G protein-coupled receptors through oligomerization. *Proc Natl Acad Sci U S A* **102**(25):8793-8794.

Footnotes

Citation of meeting abstracts: A report of these findings was presented at the 2008 annual meeting of the Biophysical Society, February 2-6, Long Beach, California.

Person to receive reprint requests: Nevin Lambert, Department of Pharmacology and Toxicology, Medical College of Georgia, Augusta, GA 30912-2300. e-mail: nlambert@mcg.edu

Figure Legends

Figure 1. Orientation and stoichiometry of coexpressed C-D2R and D2R-V. (*A*) Confocal images of live cells expressing either D2R-V or C-D2R stained with Alexa-633-conjugated anti-GFP. Only C-D2R is exposed to the antibody in intact cells; scale bar, 10 μm. (*B*) Confocal images of a single cell expressing both D2R-V and C-D2R before (*top*) and after (*bottom*) treatment with trypsin (1 mg ml^{-1}) for 1 minute; scale bar, 10 μm. (*C*) Confocal images of cells expressing C-D2R and D2R-V (*top*) or C-TM-V (*bottom*) acquired with identical settings; C excitation intensity was attenuated to normalize C-D2R and D2R-V emission intensity. The lookup table is inverted for clarity; scale bar, 10 μm. (*D*) C and V intensities measured at the plasma membrane; each point represents a single cell. The C:V ratio is higher for cells expressing C-D2R and D2R-V than for cells expressing C-TM-V.

Figure 2. Antibody crosslinking of C-D2R does not immobilize D2R-V. (*A*) Recovery of C-D2R fluorescence after photobleaching (at time=10 seconds) in cells expressing C-D2R and D2R-V is nearly abolished by anti-GFP antibody crosslinking; lines represent the mean of all experiments, grey lines represent the mean ± the s.e.m.. (*B*) Recovery of D2R-V fluorescence in the same cells as *A*. (*C-E*) Recovery of normalized fluorescence (measured at time=180 seconds) for cells expressing (*C*) C-D2R and D2R-V (control, *n*=59; anti-GFP, *n*=61), (*D*) C-D2R and β2AR-V (control, *n*=15; anti-GFP, *n*=16), and (*E*) C-TM and D2R-V (control, *n*=9; anti-GFP, *n*=9); *P<0.002; **P<0.001; bars represent mean ± s.e.m..

Figure 3. Oxidative crosslinking stabilizes C-D2R-D2RV heterooligomers via C168. (*A*) Immunoblot probed with anti-GFP primary antibody of lysates from cells transfected with equal amounts of C-D2R or D2R-V (both C168 or S168) plasmid DNA, with or without CuP treatment; the predicted molecular weight of both protomers is ~80 kDa. (*B-C*) Recovery of D2R-V fluorescence after antibody crosslinking alone (anti-GFP) or antibody and oxidative crosslinking (+CuP); lines represent the mean ± s.e.m. of all cells expressing (*B*) C-D2R C168 and D2R-V C168 or (*C*) C-D2R C168 and D2R-V S168. (*D-F*) Recovery of normalized fluorescence for cells expressing (measured at time=180 seconds) for (*D*) C-D2R C168 and D2R-V C168 (control, *n*=46; CuP, *n*=48), (*E*) C-D2R C168 and D2R-V S168 (control, *n*=25; CuP, *n*=31), and (*F*) C-D2R S168 and D2R-V C168 (control, *n*=11; CuP, *n*=17); **P<0.001; n.s. P>0.1; bars represent mean ± s.e.m..
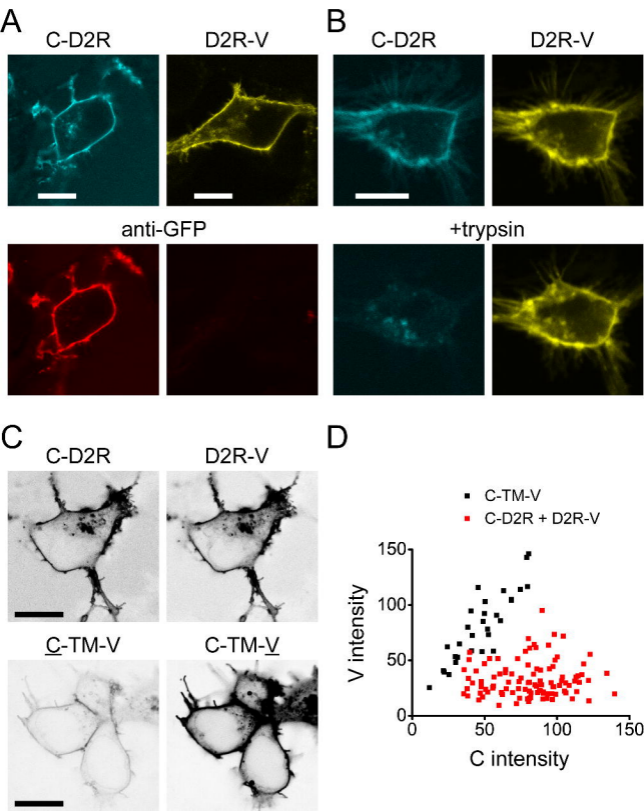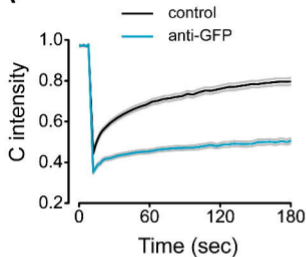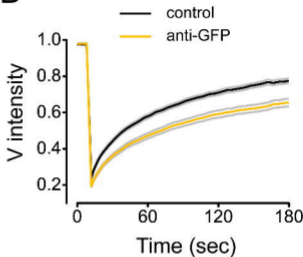
Figure 1

Figure 2

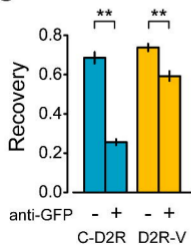# Figure 3

A

kDa

C-D2R | D2R-V

220 —

111 —
80 —

CuP   −   +   −   +   −   +   −   +
        C168   S168   C168   S168

B

D2R-V C168

V intensity

anti-GFP
+CuP

Time (sec)

C

D2R-V S168

V intensity

anti-GFP
+CuP

Time (sec)

D

Recovery

n.s.   **

CuP   −   +   −   +
     C-D2R D2R-V
     C168   C168

E

Recovery

n.s.   n.s.

CuP   −   +   −   +
     C-D2R D2R-V
     C168   S168

F

Recovery

n.s.   n.s.

CuP   −   +   −   +
     C-D2R D2R-V
     S168   C168